



# A Systematic Pan-Cancer Analysis of CASP3 as a Potential Target for Immunotherapy

Zheng Zhou<sup>1,2</sup>, Shiyong Xu<sup>1,3</sup>, Liehao Jiang<sup>1,3</sup>, Zhuo Tan<sup>1,3</sup> and Jiafeng Wang<sup>1,3\*</sup>

<sup>1</sup>Department of Head and Neck Surgery, Centre of Otolaryngology-head and Neck Surgery, Zhejiang Provincial People's Hospital, People's Hospital of Hangzhou Medical College, Hangzhou, China, <sup>2</sup>Bengbu Medical College Graduate School, Bengbu, China, <sup>3</sup>Zhejiang Provincial Key Laboratory of Diagnosis and Treatment of Endocrine Gland Diseases, Hangzhou, China

CASP3 is the gene encoding caspase-3, a specific protease that cleaves substrates such as poly-ADP ribose polymerase and acetyl-DEVD-7-amino-4-methylcoumarin. This enzymatic activity leads to DNA fragmentation, which is a hallmark of apoptosis. Although recent studies have demonstrated that CASP3 plays a vital role in tumour suppression by promoting apoptosis, these reports did not consider systematic pan-cancer analyses. Therefore, we performed a specific pan-cancer analysis using The Cancer Genome Atlas and Genotype-Tissue Expression databases to analyse CASP3 expression in terms of cancer prognosis, DNA methylation status, tumour mutative burden (TMB), and microsatellite instability (MSI), as well as immune cell infiltration in different tumours and the molecular mechanisms underlying these. We found that CASP3 expression was significantly associated with the prognosis of most tumours. Additionally, promoter methylation status was associated with CASP3 expression in bladder urothelial carcinoma, oesophageal carcinoma, kidney renal clear cell carcinoma, kidney renal papillary cell carcinoma, lung squamous cell carcinoma, prostate adenocarcinoma, sarcoma, testicular germ cell tumours, and uterine corpus endometrial carcinoma. TMB and MSI were associated with CASP3 expression in 15 tumours. Moreover, CASP3 expression was correlated with the tumour microenvironment in nearly all tumour types. Further, we observed that in addition to apoptosis, CASP3 action plausibly involves B cell activation, antigen presentation, immune responses, chemokine receptors, and inflammatory function. Our study thus provides a relatively comprehensive understanding of the carcinogenicity of CASP3 in different tumours and suggests that CASP3 is a potential prognostic marker.

**Keywords:** CASP3, cancer, prognosis, immune infiltration, tumor microenvironment

## INTRODUCTION

Epidemiological studies have shown that global cancer incidence is increasing annually, being expected to surpass coronary artery disease as the leading cause of death worldwide by 2060 (Mattiuzzi and Lippi, 2019). In recent years, remarkable progress has been made in tumour immunotherapy, and an increasing number of immunotherapy drugs have been approved for clinical use (Bulk et al., 2018). However, there is no definitive treatment for cancer. With the development of many clinical databases, such as The Cancer Genome Atlas (TCGA),

## OPEN ACCESS

### Edited by:

Qi Zhao,  
University of Science and Technology  
Liaoning, China

### Reviewed by:

Udayan Bhattacharya,  
NewYork-Presbyterian, United States  
Zhan Wang,  
Zhejiang University, China

### \*Correspondence:

Jiafeng Wang  
wangjiafeng@hmc.edu.cn

### Specialty section:

This article was submitted to  
Molecular Diagnostics and  
Therapeutics,  
a section of the journal  
Frontiers in Molecular Biosciences

**Received:** 05 November 2021

**Accepted:** 02 March 2022

**Published:** 29 April 2022

### Citation:

Zhou Z, Xu S, Jiang L, Tan Z and  
Wang J (2022) A Systematic Pan-  
Cancer Analysis of CASP3 as a  
Potential Target for Immunotherapy.  
Front. Mol. Biosci. 9:776808.  
doi: 10.3389/fmolb.2022.776808

pan-cancer analysis has facilitated exploration of related pathways and molecular mechanisms in specific tumours and the evaluation of their effects on prognosis. Thus, an emerging trend in tumour therapy includes identifying new potential therapeutic targets in addition to traditional surgical therapy (Blum et al., 2018).

Caspase-3 (CASP3) is a key enzyme in the apoptotic pathway that plays an important role in tumorigenesis and cancer progression (Crowley and Waterhouse, 2016). Thus, CASP3 activation is often used by researchers as an alternative marker to evaluate the efficacy of cancer treatments. However, numerous studies have indicated that CASP3 does not simply inhibit tumour growth, whereas others have reported that CASP3 activation after chemical or radiation exposure may be associated to carcinogenesis (Liu et al., 2015). Several studies have shown that CASP3 promotes tumour growth by creating a microenvironment that promotes angiogenesis (Feng et al., 2017; Bernard et al., 2019). In a colon cancer study, CASP3 was found to play a role in tumour invasion and metastasis, and the deletion of CASP3 often indicates higher sensitivity to chemotherapy and radiation, suggesting that cleaved CASP3 may serve as a new therapeutic target in cancer (Zhou et al., 2018).

However, related studies have not sufficiently elucidated the mechanisms of apoptosis, and the specific role of CASP3 in different tumours remains unclear. Therefore, we used the TCGA, Genotype-Tissue Expression (GTEx), and other databases to conduct a specific pan-cancer analysis of CASP3. In addition to CASP3 expression in different tumours and its prognostic implications, our analysis included gene mutations, methylation, tumour mutational burden (TMB), microsatellite instability (MSI), and potential associations of CASP3 in 33 tumour types. Regarding the tumour microenvironment, fibroblast and immune cell infiltration, co-expression of CASP3, and related pathways were also analysed. Our findings may provide foundation for new strategies for the treatment of related tumours.

## MATERIALS AND METHODS

### Data Processing and Differential Expression Analysis

Using UCSC Xena (<https://Xena.UCSC.edu/>), an online tool for exploring gene expression and clinical and phenotypic data, we downloaded the RNA sequence, somatic mutation, and related clinical data from the TCGA (comprising 10,201 samples from 33 types of cancer). Gene expression data from 31 different normal tissues were downloaded from the GTEx database (<https://commonfund.nih.gov/GTEx>). All gene expression data were normalised using  $\log_2$  transformation. Normal and cancer tissues were compared using the *t*-test. The Kaplan-Meier curve, logarithmic rank test, and Cox proportional hazard model were used in all survival analyses. The correlation between variables were calculated using the Spearman or Wilcoxon tests. All statistical analyses were performed using R software (version 4.0.2 or

3.6.3, <https://www.r-project.org>). Statistical significance was set at  $p < 0.05$ .

### Gene Expression Analysis

We entered “CASP3” in the tumour immune estimation resource (TIMER2) “Gene DE” module (version 2, <http://timer.cistrome.org/>) to investigate the differences in CASP3 expression among different tumours or specific tumour subtypes in the TCGA data using tumour and adjacent normal tissues. Certain tumours did not have the corresponding normal tissue samples or displayed lower expression in normal tissues. Under these conditions, we entered “CASP3” in the gene expression profiling interactive analysis (GEPIA2; <http://gepia2.cancer-pku.cn/#index>), an online tool for gene expression and co-expression analysis, in the “DIY Expression” module’s “Box plot”, with the following parameters: *p*-value cut-off = 0.01,  $\log_2$ FC (fold change) cut-off = 1,  $\log_2$  (TPM + 1) for log-scale, and “Match TCGA Normal and GTEx”, and obtained the differential scatter plot and the expression bodymap of CASP3 between tumours and corresponding normal tissues in the GTEx database. The UALCAN portal (<http://ualcan.path.uab.edu/analysis-prot.html>) is an online tool for the proteomic analysis of several types of cancer. We used the Clinical Proteomic Tumour Analysis Consortium (CPTAC) dataset for protein expression analysis. We analysed the expression of CASP3 in tumour and normal tissues by inputting “CASP3”. Six available tumour datasets were selected, namely breast, ovarian, colon, clear cell renal cell carcinoma (RCC), UCEC, and lung adenocarcinoma (LUAD). Subsequently, to evaluate the difference in CASP3 expression at the protein level, we downloaded and compared the immunohistochemistry (IHC) images for CASP3 protein in normal tissues and six tumour tissues from the Human Protein Atlas (HPA; <http://www.proteinatlas.org/>).

### Prognostic Survival Analysis

By combining gene expression and clinical data from each sample extracted from the TCGA database, the relationship between the CASP3 expression and patient prognosis was studied using four indices: overall survival (OS), disease-specific survival (DSS), disease-free interval (DFI), and progression-free interval (PFI). Kaplan-Meier and log-rank tests were used for the survival analysis ( $p < 0.05$ ). The prognostic data were visualised using R software (version 3.6.3), with the R packages “survival” and “survminer”. In addition, the Cox analysis used the R packages “survival” and “forestplot” to determine the pan-cancer relationship between CASP3 expression and survival. We then obtained the stage differences of CASP3 in different tumours using the GEPIA2 “Stage plot” module and constructed the relevant violin plots using  $\log_2$ [TPM + 1].

### Gene Methylation Analysis

We entered the gene “CASP3” in the UALCAN portal and analysed the differences in methylation expression in tumour and normal tissues. Thereafter, we used SurvivalMeth (<http://bio-bigdata.hrbmu.edu.cn/survivalmeth/>), an online tool for studying the effect of gene methylation on prognosis, with the parameters set as Method “T-test” and “Threshold Value” = 0.01, the

“Maxstat” grouping strategy, and the remaining settings at “Without Restriction” to obtain the effect of *CASP3* methylation levels on overall survival in TCGA database and the Kaplan-Meier survival curve with a statistically significant  $p$ -value ( $p < 0.05$ ).

## Gene Mutation Analysis

On the cBioPortal website (<https://www.cbioportal.org/>), an interactive exploration dataset for multiple cancer genomics, we selected “TCGA PanCancer Atlas study” in the “Quick By Gene” and entered “*CASP3*” to query for genetic mutation-related characteristics of *CASP3*. Mutation-related results were observed in all the TCGA tumours in the “Cancer Type Summary” module. Information regarding the *CASP3* mutation site can be displayed in a protein structure sketch map or three-dimensional (3D) structure using the “Mutation” module. We also used the “Comparison/Survival” module to obtain OS, DSS, DFI, and PFI data for TCGA cancer cases with more *CASP3* mutations and generated the Kaplan-Meier survival curve. TMB is defined as the total number of somatic gene coding, base insertion, replacement, or deletion errors detected per million bases (Yarchoan et al., 2017), which is an important biological indicator of the extent of mutation in tumours; a higher TMB often indicates better outcomes for tumour immunotherapy (Le et al., 2015). The MSI results were obtained as a result of functional defects in DNA mismatch repair in tumour tissues, and MSI-H tumours often imply better treatment outcomes (Lin et al., 2020). We then analysed the association between *CASP3* expression and TMB using mutation data from the TCGA database, derived from the 2018 study by Thorsson et al. (Thorsson et al., 2018) using R software (version 4.0.3);  $p < 0.05$  was considered statistically significant. We simultaneously analysed the correlation between *CASP3* expression and MSI data obtained from the study by Bonneville et al. (Bonneville et al., 2017).

## Tumour Microenvironment Analysis

Before analysing the tumour microenvironment, we first analysed the correlation between the expression of *CASP3* and eight immunologic checkpoints (*SIGLEC15*, *ID O 1*, *CD274*, *Havcr2*, *PDCD1*, *CTLA4*, *LAG3*, and *PDCD1LG2*). The expression values of these eight genes and *CASP3* in all tumours were extracted, and a correlation heatmap was visualised using R software (version 4.0.3). We used “the cancer-associated fibroblast” module in TIMER2 to explore the relationship between *CASP3* expression and fibroblast infiltration, and used the EPIC, MCP-counter, and TIDE algorithms to evaluate the data, which were visualised as a heatmap and scatter plot. Thereafter, we used the “Outcome” module of TIMER2 to analyse the prognosis and obtain the Kaplan-Meier survival curve with  $p < 0.05$ . We then used the previously downloaded mRNA data from TCGA database and the latest algorithms from TIMER, xCell, MCP-counter, CIBERSORT, EPIC, and quanTIseq with the R package “ImmuneDeconv” (R software, version 4.0.3) (Sturm et al., 2020) to perform immune infiltration analysis and evaluate the correlation between *CASP3* expression and infiltration of immune cells in different tumours, which was

then visualised as a heatmap. The Kaplan-Meier curve was obtained using the same methods.

## Tumour Enrichment Analysis

Gene Ontology (GO) and Kyoto Encyclopaedia of Genes and Genomes (KEGG) gene sets were downloaded from the GSEA website (<https://www.GSEA-msigdb.org/GSEA/downloads.jsp>). Functional analysis was performed using the R software (version 3.6.3) packages “Limma”, “Org.Hs.eg.db”, “DOSE”, “ClusterProfiler”, and “Enrich plot” to visualise the five most significant *CASP3* enrichment pathways in different tumours.  $p < 0.05$  was considered statistically significant.

## CASP3-Related Gene Enrichment Analysis

We used the gene name “*CASP3*” and the “*Homo sapiens*” condition to search the STRING database (<https://string-db.org/>) with the parameter minimum required interaction score (“Low confidence (0.150)”), meaning of network edges (“evidence”), and max number of interactors (“no more than 50 interactors” in 1st shell), to obtain the *CASP3*-associated protein network map. Next, we used the GEPIA2 “Similar gene detection” module based on TCGA and GTEx datasets to obtain the first 100 genes closely related to *CASP3*. In addition, the co-expression of *CASP3* and related genes in different tumours was plotted using the R package “Limma” (R software, version 3.6.3). Thereafter, *CASP3* and the selected genes, namely *DDX46*, *GNAI3*, *PDS5A*, *SCYL2*, and *TMPO*, were analysed using “Correlation analysis” in GEPIA2 and a scatter plot was obtained. We used two sets of data to perform the GO and KEGG enrichment analysis and used R software (version 4.0.3) and the packages “ClusterProfiler”, “Org.Hs.eg.db”, “Enrichplot”, and “ggplot2” to visualise the data as bubble plots. The first five correlation pathways were selected to draw the loop plot of the related genes.

## RESULTS

### Gene Expression Analysis Data

We first analysed the differential expression of *CASP3* among different tumours in the TCGA database using the TIMER2 method (Figure 1A). We observed a statistically significant overexpression in bladder urothelial carcinoma (BLCA), breast invasive carcinoma (BRCA), cervical squamous cell carcinoma and endocervical adenocarcinoma (CESC), cholangiocarcinoma (CHOL), oesophageal carcinoma (ESCA), kidney renal clear cell carcinoma (KIRC), kidney renal papillary cell carcinoma (KIRP), lung squamous cell carcinoma (LUSC), glioblastoma multiforme (GBM), head and neck squamous cell carcinoma (HNSC), liver hepatocellular carcinoma (LIHC), lung adenocarcinoma (LUAD), stomach adenocarcinoma (STAD), thyroid carcinoma (THCA), and uterine corpus endometrial carcinoma (UCEC). For tumours with no or few corresponding normal tissue samples, such as lymphoid neoplasm, diffuse large B-cell lymphoma (DLBC), brain lower grade glioma (LGG), *CASP3* as a negative expression of colon adenocarcinoma (COAD), and rectum adenocarcinoma (READ), we used normal tissue

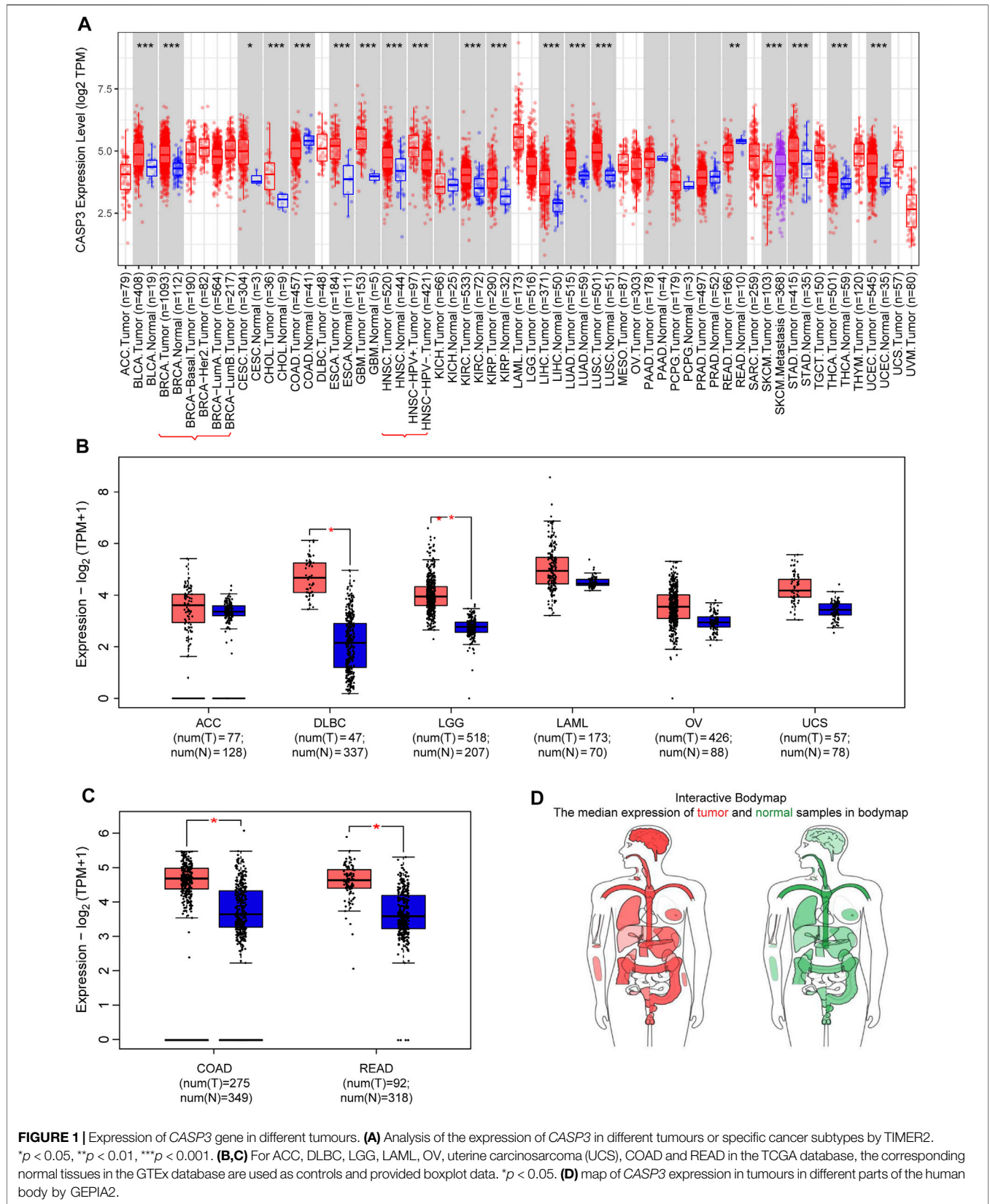
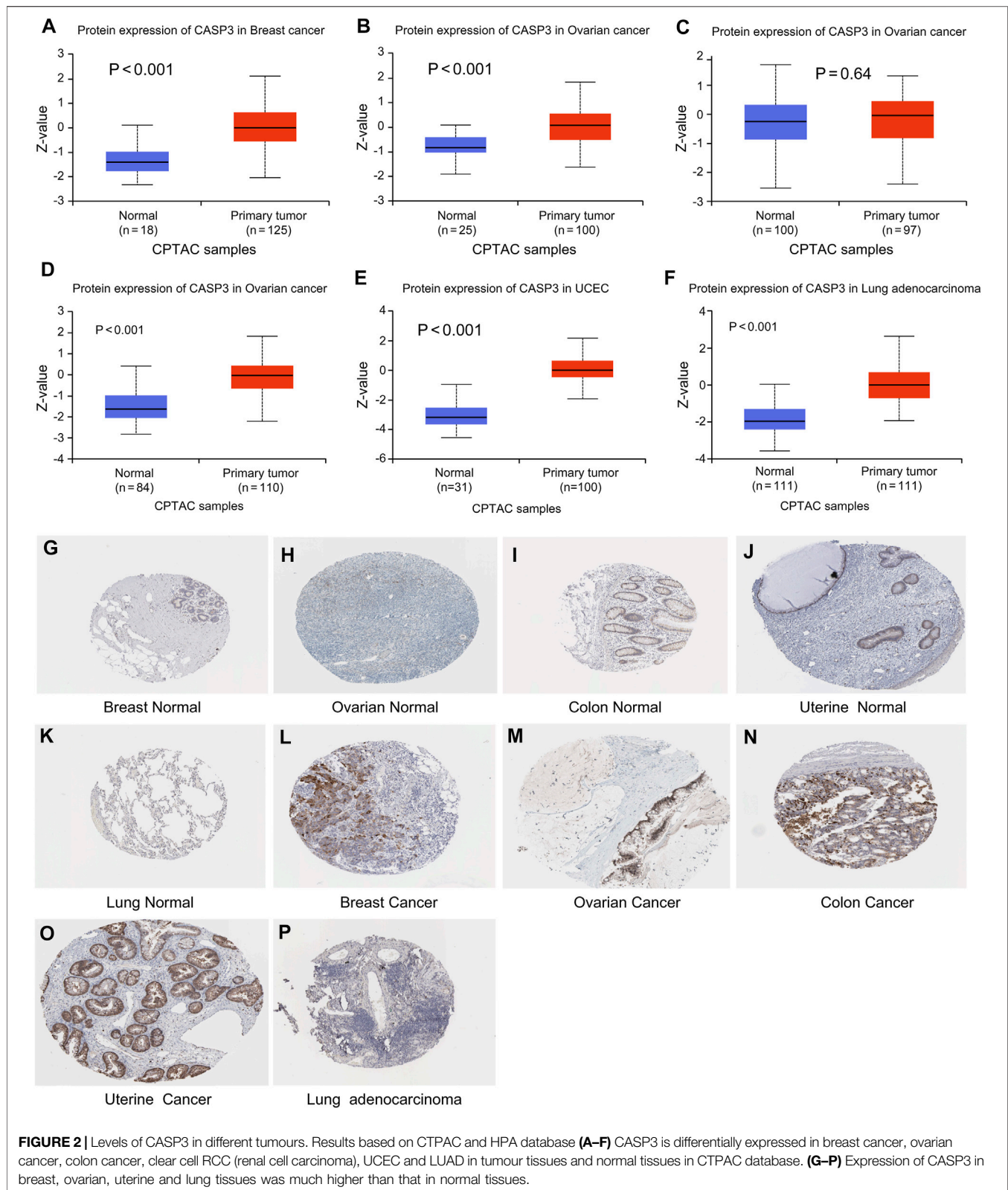
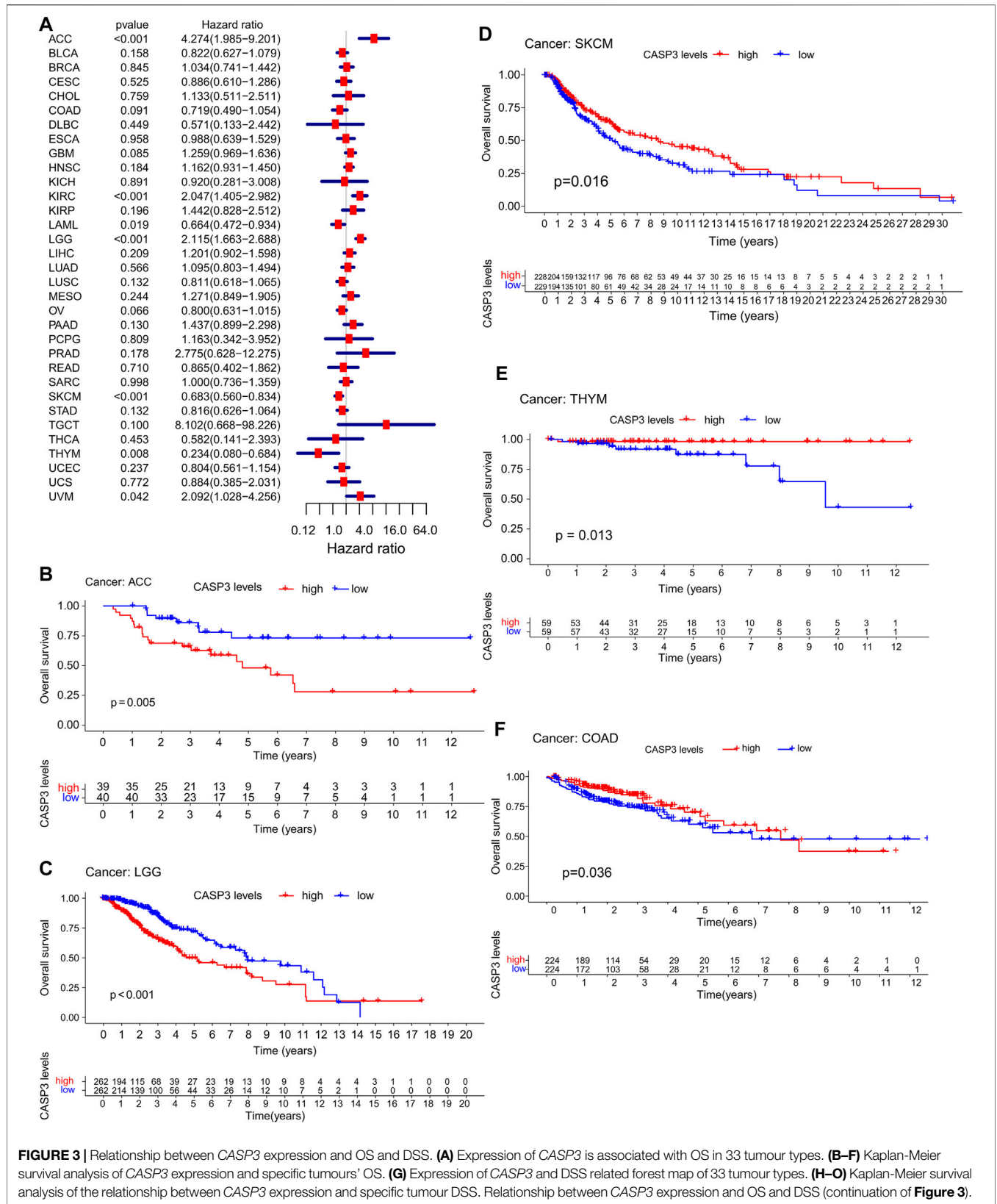


**FIGURE 1** | Expression of CASP3 gene in different tumours. **(A)** Analysis of the expression of CASP3 in different tumours or specific cancer subtypes by TIMER2. \**p* < 0.05, \*\**p* < 0.01, \*\*\**p* < 0.001. **(B,C)** For ACC, DLBC, LGG, LAML, OV, uterine carcinosarcoma (UCS), COAD and READ in the TCGA database, the corresponding normal tissues in the GTEx database are used as controls and provided boxplot data. \**p* < 0.05. **(D)** map of CASP3 expression in tumours in different parts of the human body by GEPIA2.



expression from the GTEx database added to GEPIA2 to analyse the results (**Figures 1B,C**). In previously negative and non-normal tumours, CASP3 expression was significantly higher in

DLBC, LGG, COAD, and READ tissues compared with that in normal tissues ( $p < 0.001$ ). CASP3 expression was high in almost all other human tumours (**Figure 1D**).



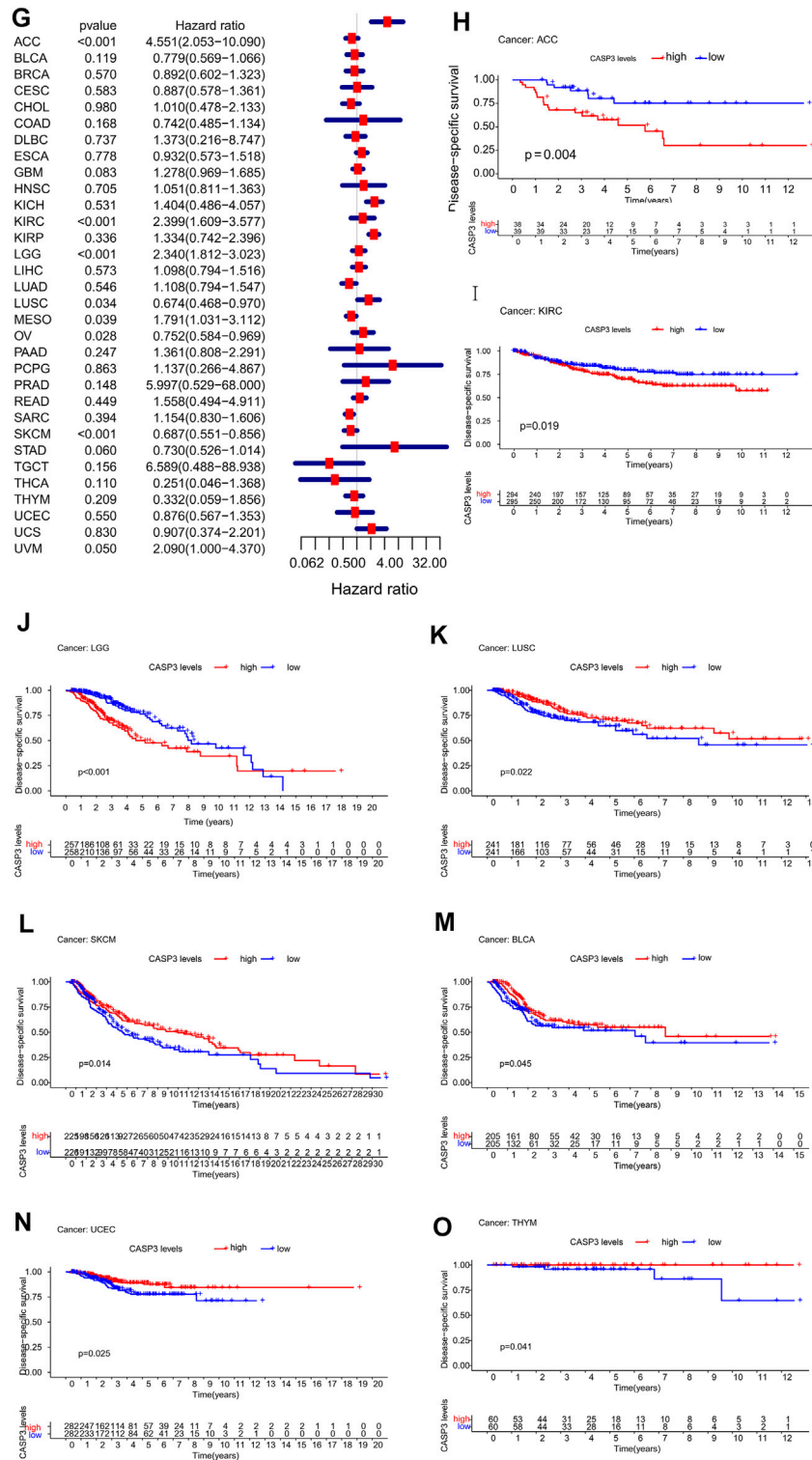


FIGURE 3 | (Continued).

Subsequently, to evaluate CASP3 expression at the protein level, we analysed the results of IHC staining in the HPA database and compared them with the levels of protein expression in six

tumours obtained from the CPTAC database. The expression of CASP3 protein was significantly higher in all tumours, except in the colon ( $p < 0.001$ , **Figures 2A-F**). The remaining images

indicate CASP3 IHC staining in normal tissues (**Figures 2G–K**) and in five tumours (**Figures 2L–P**). Unfortunately, no staining results have been reported for clear cell RCC. CASP3 IHC staining was low in normal tissues of the breast, uterus, ovary, and lung, and was moderate in normal tissues of the colon. Breast cancer and ovarian cancer tissues showed strong staining whereas colon cancer, UCEC, and LUAD tissues all showed moderate staining; with the exception of the colon, CASP3 protein expression in tumour tissues was significantly higher than that in normal tissues, which was consistent with the results obtained from the CPTAC database.

## Prognostic Analysis Data

Concerning prognosis, we performed survival association analysis for each tumour type, including OS, DSS, DFI, and PFI data. The Cox model of OS rate showed that CASP3 expression was correlated with adrenocortical carcinoma (ACC,  $p < 0.001$ ), KIRC ( $p < 0.001$ ), acute myeloid leukaemia (LAML,  $p = 0.019$ ), LGG ( $p < 0.001$ ), SKCM ( $p < 0.001$ ), thymoma (THYM,  $p = 0.008$ ), and uveal melanoma (UVM,  $p < 0.042$ , **Figure 3A**). CASP3 was identified as a high-risk gene in ACC, KIRC, LGG, and UVM, particularly in ACC, with a hazard ratio of 4.274, whereas it was a low-risk gene in the remaining tumours. Kaplan-Meier survival analysis also showed that high CASP3 expression in ACC ( $p = 0.005$ , **Figure 3B**) and LGG ( $p < 0.001$ , **Figure 3C**) was associated with low OS, whereas high CASP3 expression in SKCM ( $p = 0.016$ , **Figure 3D**), THYM ( $p = 0.013$ , **Figure 3E**), and COAD ( $p = 0.036$ , **Figure 3F**) was associated with better prognosis.

Furthermore, in DSS, high CASP3 expression in ACC ( $p < 0.001$ ), KIRC ( $p < 0.001$ ), LGG ( $p < 0.001$ ), mesothelioma (MESO,  $p = 0.039$ ), and UVM ( $p = 0.05$ ) was associated with poor prognosis (**Figure 3G**). However, we observed opposing results in LUSC ( $p = 0.034$ ), ovarian serous cystadenocarcinoma (OV,  $p = 0.028$ ), and SKCM ( $p < 0.001$ ). Kaplan-Meier survival analysis showed that high CASP3 expression was not only associated with poor prognosis in ACC ( $p = 0.004$ , **Figure 3H**), KIRC ( $p = 0.019$ , **Figure 3I**), and LGG ( $p < 0.001$ , **Figure 3J**) but also with the prognosis of LUSC ( $p = 0.022$ , **Figure 3K**), SKCM ( $p = 0.014$ , **Figure 3L**), BLCA ( $p = 0.045$ , **Figure 3M**), UCEC ( $p = 0.025$ , **Figure 3N**), and THYM ( $p = 0.041$ , **Figure 3O**). In DFI (**Figure 4A**), in contrast to the CASP3-related good prognosis in OV ( $p = 0.013$ ), CASP3 overexpression was associated with poor prognosis in ACC ( $p = 0.008$ ), KIRC ( $p = 0.048$ ), LUAD ( $p = 0.005$ ), and THCA ( $p < 0.001$ ). The Kaplan-Meier survival analysis showed the same results for OV ( $p = 0.012$ , **Figure 4B**), with a good prognosis, whereas the prognoses of ACC ( $p = 0.012$ , **Figure 4C**), BLCA ( $p = 0.009$ , **Figure 4D**), KIRC ( $p = 0.012$ , **Figure 4E**), and LUAD ( $p = 0.005$ , **Figure 4F**) were poor. Finally, high CASP3 expression was associated with low PFI in ACC ( $p < 0.001$ ), KIRC ( $p = 0.018$ ), LGG ( $p < 0.001$ ), LUAD ( $p = 0.044$ ), prostate adenocarcinoma (PRAD;  $p = 0.002$ ), and UVM ( $p = 0.002$ , **Figure 4G**). Kaplan-Meier survival analysis showed that the high CASP3 expression was associated with poor prognosis in ACC ( $p < 0.001$ , **Figure 4H**), LUAD ( $p = 0.029$ , **Figure 4I**), LGG ( $p = 0.001$ ,

**Figure 4J**), PRAD ( $p = 0.017$ , **Figure 4K**), and KIRC ( $p = 0.036$ , **Figure 4L**); high CASP3 expression was also associated with poor prognosis in sarcoma (SARC;  $p = 0.016$ , **Figure 4M**) and good prognosis in READ ( $p = 0.006$ , **Figure 4N**), COAD ( $p = 0.028$ , **Figure 4O**). Further, we used the “Stage Plot” module of GEPIA2 to observe the relationship between CASP3 expression and the pathological staging of tumours. We observed correlations between the expression of CASP3 and COAD (**Figure 4P**), SKCM (**Figure 4Q**), OV (**Figure 4R**), and THCA (**Figure 4S**,  $p < 0.05$ ). The remaining tumours are shown in **Supplementary Figure S1**.

## Genetic Methylation Analysis Data

First, we analysed the differences in CASP3 methylation levels in TCGA using the UALCAN database. In ESCA (**Figure 5B**), KIRC (**Figure 5C**), LUSC (**Figure 5D**), and SARC (**Figure 5G**), CASP3 methylation levels were high, whereas in BLCA (**Figure 5A**), PRAD (**Figure 5E**), KIRC (**Figure 5F**), testicular germ cell tumours (TGCT; **Figure 5H**), and UCEC (**Figure 5I**), the reverse was true. We then used the “Single Case” plate of SurvivalMeth to analyse the relationship between CASP3 methylation and tumour prognosis in TCGA database and obtain the Kaplan-Meier survival curve. Despite tumours that could not be analysed effectively because of lack of data, we observed that CASP3 methylation levels only in ESCA ( $p = 0.047$ , **Figure 5K**) indicated a good prognosis, whereas in BLCA ( $p = 0.027$ , **Figure 5J**), KIRC ( $p = 0.010$ , **Figure 5L**), and LUSC ( $p < 0.001$ , **Figure 5M**), CASP3 methylation levels were correlated with poor prognosis ( $p < 0.05$ ). The levels of methylation in the other tumours and the associated prognoses are shown in **Supplementary Figure S2**.

## Gene Mutation Analysis Data

We observed genetic changes in CASP3 in different TCGA tumours using cBioPortal. The highest frequency of CASP3 mutations was 3% in UCEC (**Figure 6A**). In DLBC, “deep deletion” highlighted the full range of mutations (>8%). Notably, almost all tumours with mutations had a missing copy number of CASP3. All genetic loci of CASP3 and the number of cases are shown in **Figure 6B**. The missense mutation of CASP3 was the main type of genetic change, accounting for more than 80% of cases. In all three cases, mutations at R147C were detected in SKCM. A 3D map of CASP3 mutations at this site is shown in **Figure 6C**. In addition, we continued to explore the relationship between CASP3 mutations and clinical survival. In DLBC, CASP3 mutations resulted in poor OS ( $p = 0.005$ , **Figure 6D**), DSS ( $p = 0.006$ , **Figure 6E**), and PFI ( $p = 0.04$ , **Figure 6F**), therefore, it was chosen for the analysis as it had the most mutations. However, for DFI ( $p = 0.7$ , **Figure 6G**), which was not statistically significant because there was only one case of mutation data.

We also analysed the association of CASP3 expression with TMB and MSI in all tumours in TCGA database. In STAD ( $p < 0.001$ ), UCEC ( $p < 0.001$ ), BRCA ( $p < 0.001$ ), ACC ( $p = 0.002$ ), COAD ( $p = 0.002$ ), LGG ( $p = 0.002$ ), PRAD ( $p = 0.015$ ), and



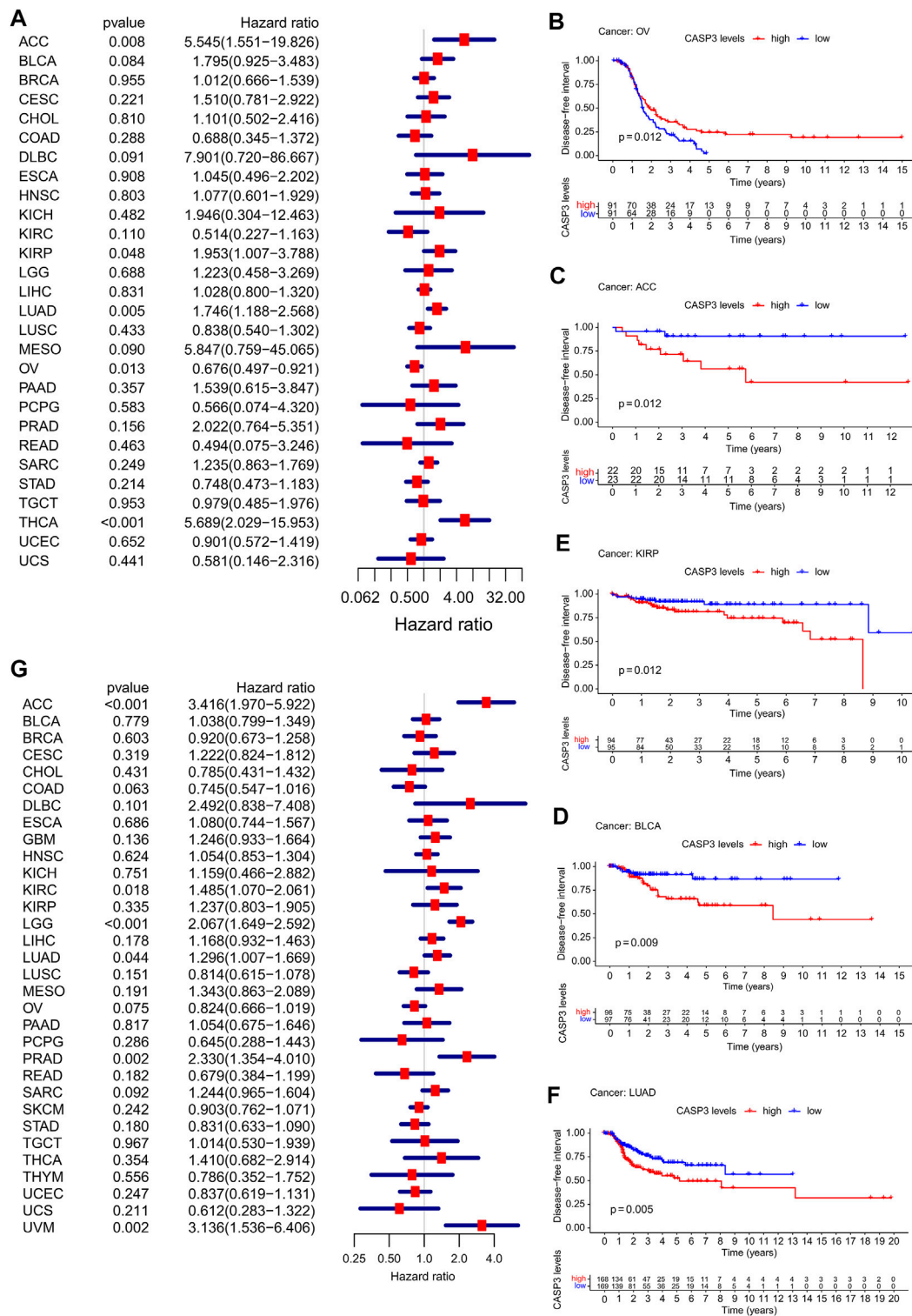


**FIGURE 4 |** Relationship between CASP3 expression and DFI, PFI, and different pathological stages. **(A)** Expression of CASP3 is associated with DFI in 33 tumour types. **(B–F)** Kaplan-Meier survival analysis of the relationship between expression of CASP3 and DFI in specific tumours. **(G)** Forest map of correlation between expression of CASP3 and PFI in 33 tumour types. **(H–O)** Kaplan-Meier survival analysis of the relationship between the expression of CASP3 and PFI in specific tumours. **(P–S)** Relationship between CASP3 levels and different pathological stages of COAD, SKCM, THCA, OV. Relationship between CASP3 expression and DFI, PFI, and different pathological stages (continuation of **Figure 4**).

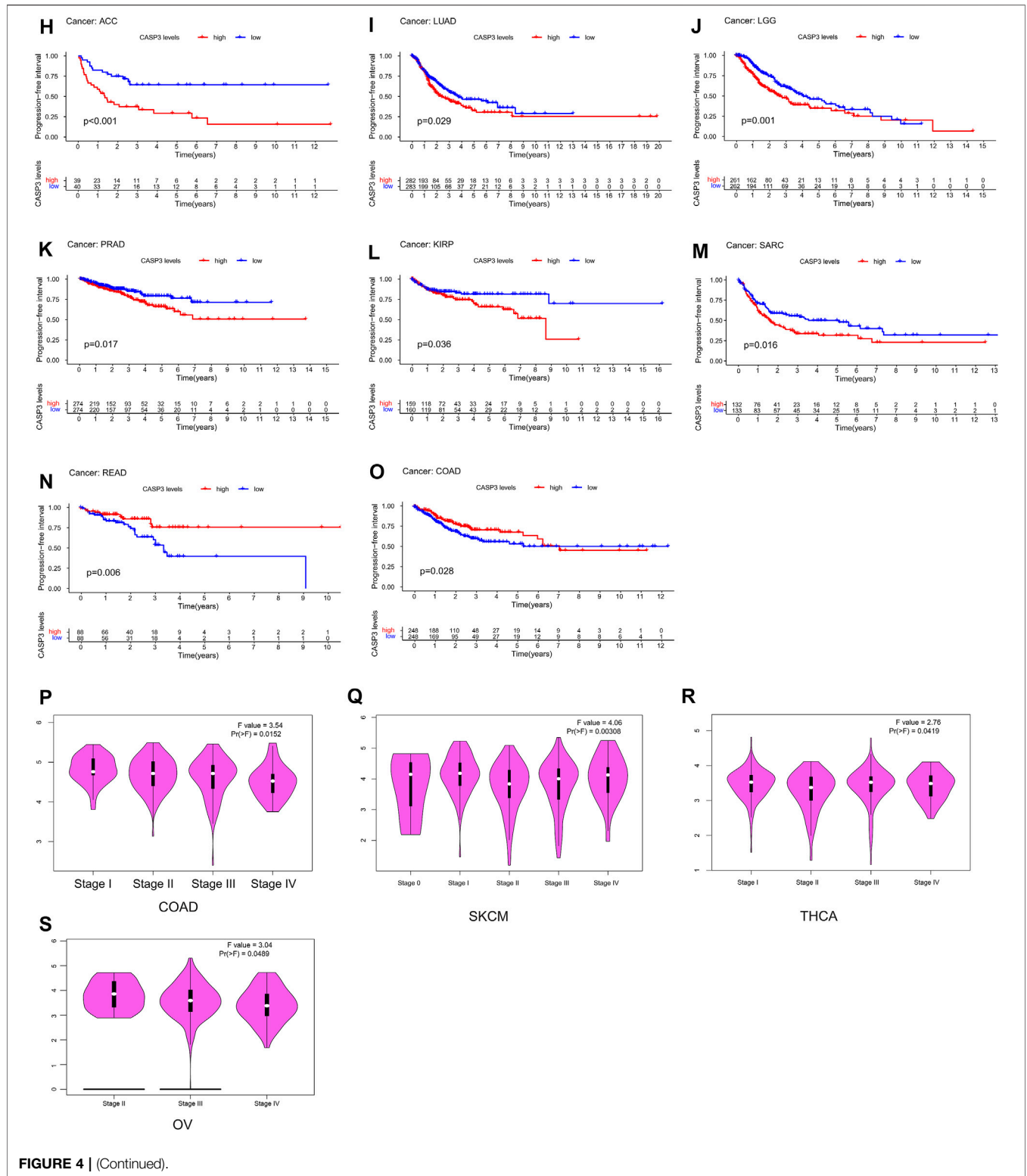
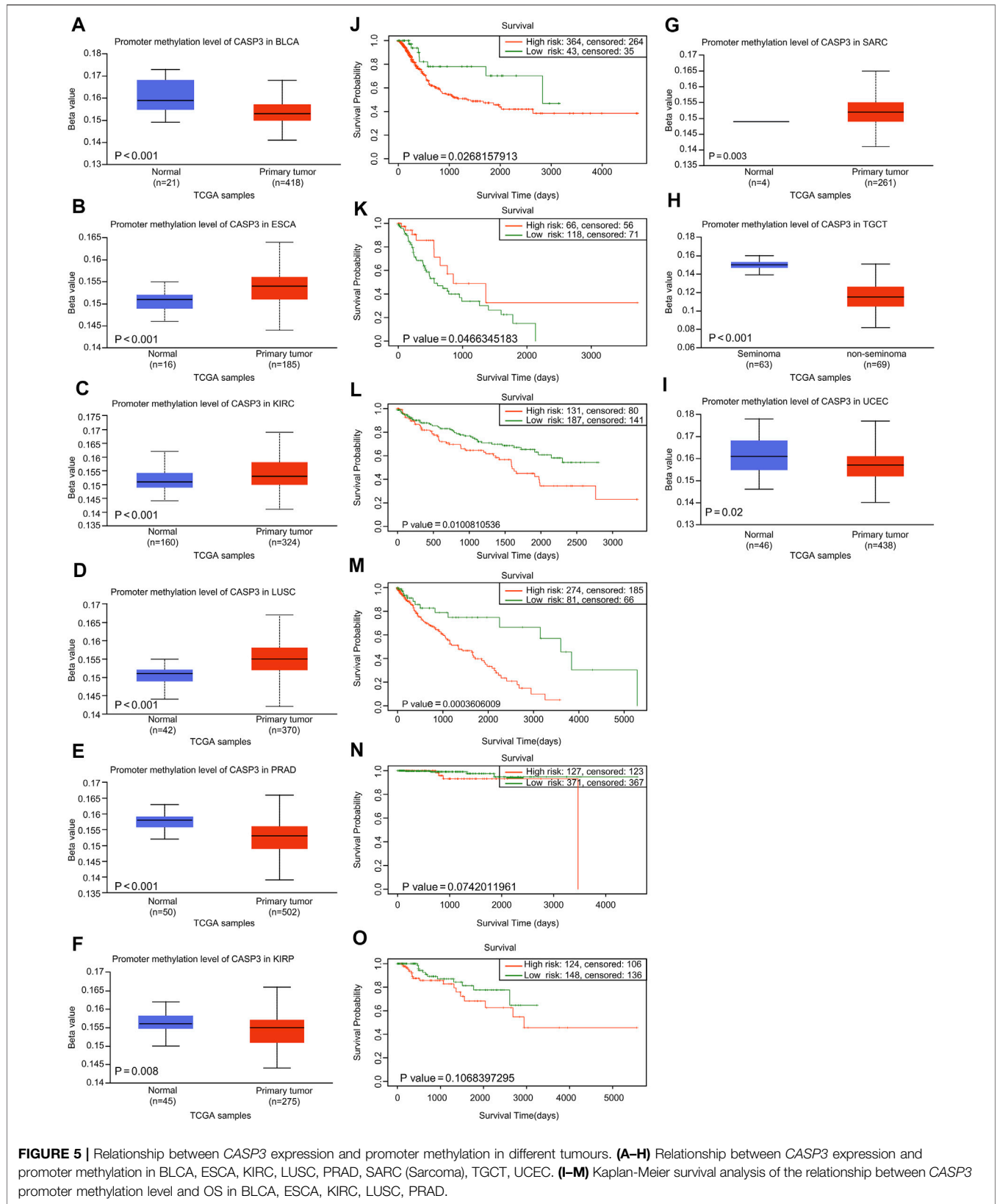


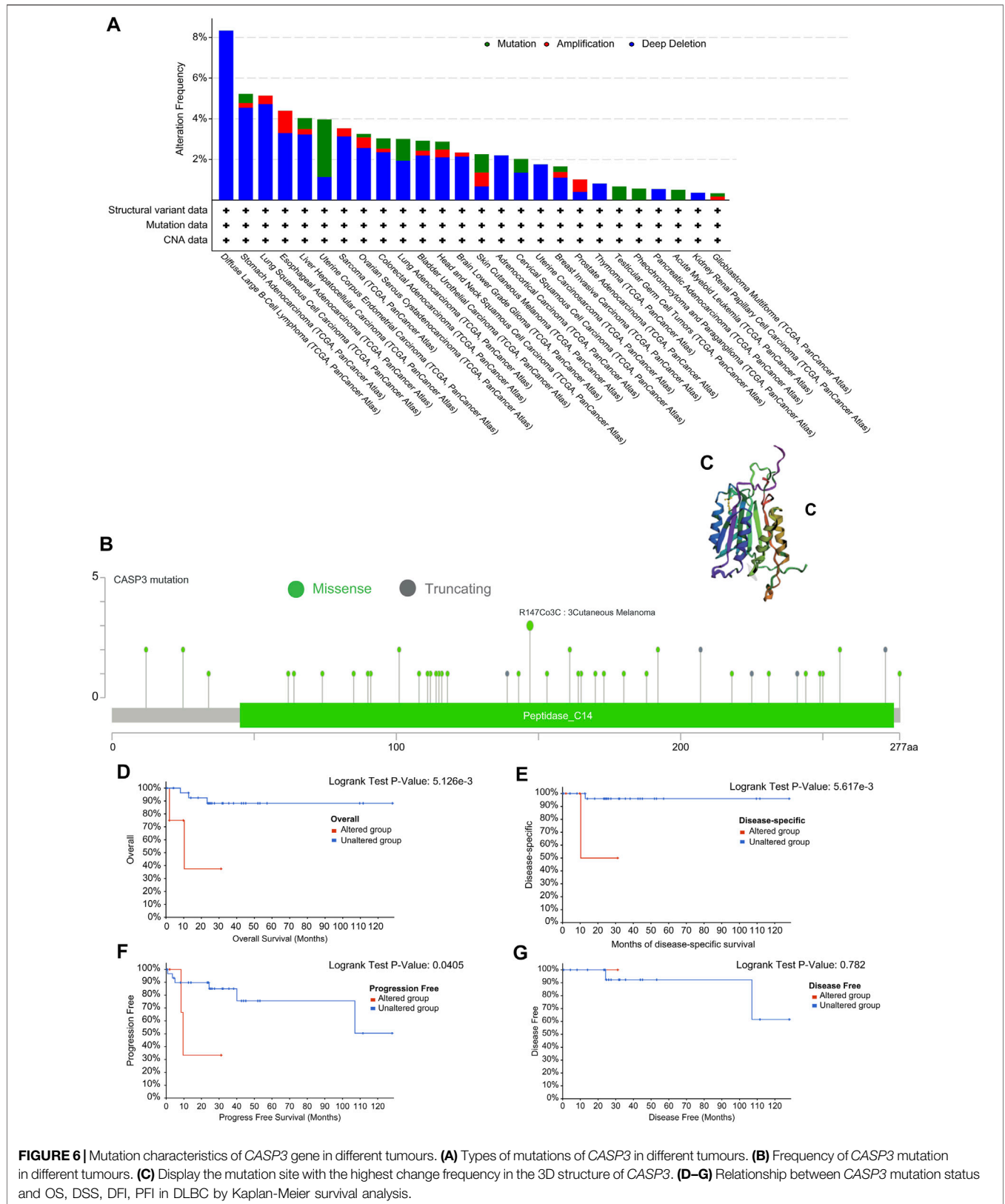
FIGURE 4 | (Continued).

pancreatic adenocarcinoma (PAAD,  $p = 0.025$ ), *CASP3* expression was positively correlated with TMB, whereas was negatively correlated in UVM ( $p = 0.003$ ), THCA ( $p < 0.001$ ), and LIHC ( $p = 0.044$ , **Figure 7A**). In READ ( $p = 0.001$ ), UCEC

( $p < 0.001$ ), STAD ( $p < 0.001$ ), and KIRC ( $p = 0.019$ ), *CASP3* expression was positively correlated with MSI, but was negatively correlated with MSI in DLBC ( $p = 0.008$ ) and LUAD ( $p = 0.03$ , **Figure 7B**).



**FIGURE 5 |** Relationship between CASP3 expression and promoter methylation in different tumours. **(A–H)** Relationship between CASP3 expression and promoter methylation in BLCA, ESCA, KIRC, LUSC, PRAD, SARC (Sarcoma), TGCT, UCEC. **(I–M)** Kaplan-Meier survival analysis of the relationship between CASP3 promoter methylation level and OS in BLCA, ESCA, KIRC, LUSC, PRAD.



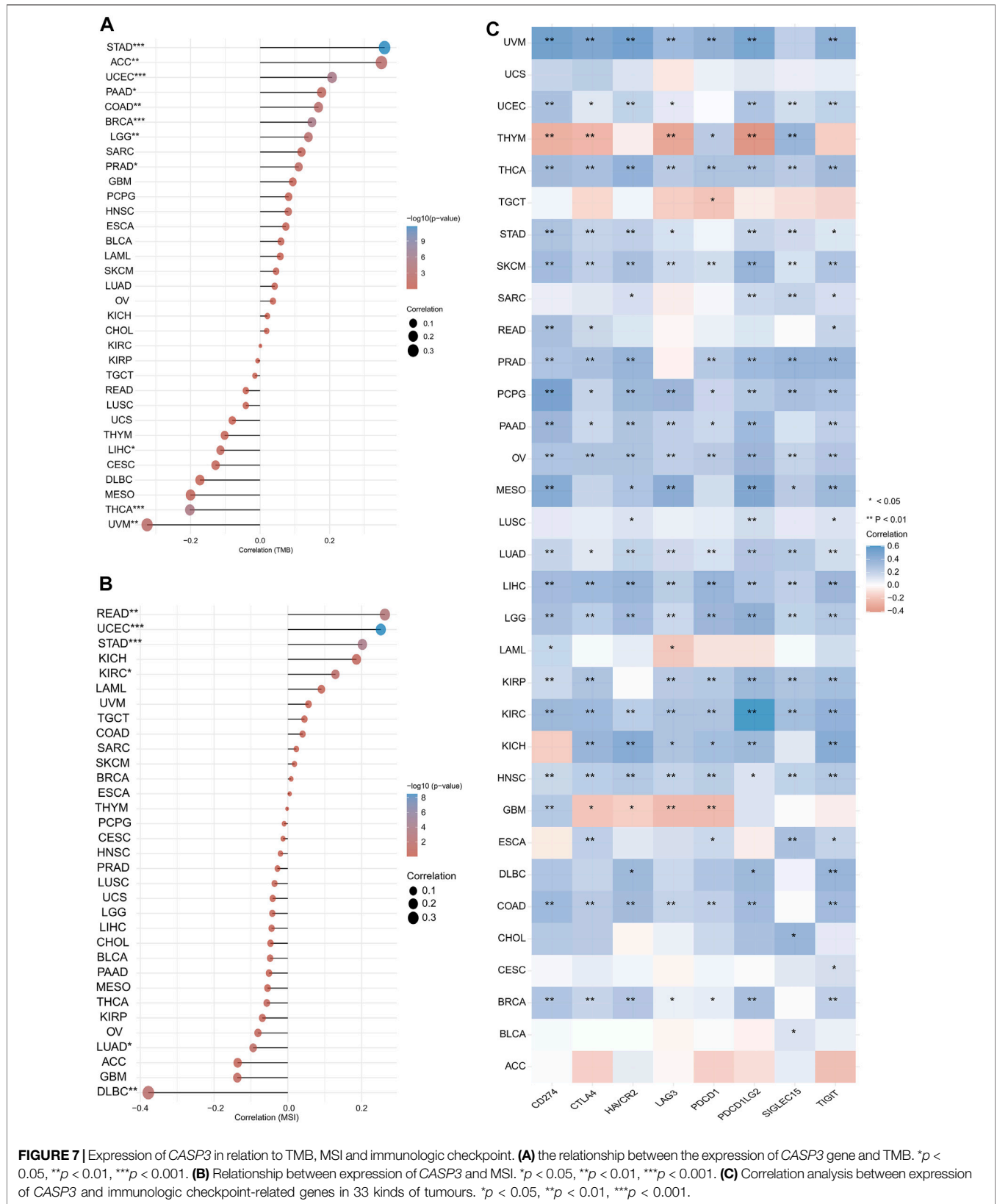


**FIGURE 7 |** Expression of *CASP3* in relation to TMB, MSI and immunologic checkpoint. **(A)** the relationship between the expression of *CASP3* gene and TMB. \* $p < 0.05$ , \*\* $p < 0.01$ , \*\*\* $p < 0.001$ . **(B)** Relationship between expression of *CASP3* and MSI. \* $p < 0.05$ , \*\* $p < 0.01$ , \*\*\* $p < 0.001$ . **(C)** Correlation analysis between expression of *CASP3* and immunologic checkpoint-related genes in 33 kinds of tumours. \* $p < 0.05$ , \*\* $p < 0.01$ , \*\*\* $p < 0.001$ .

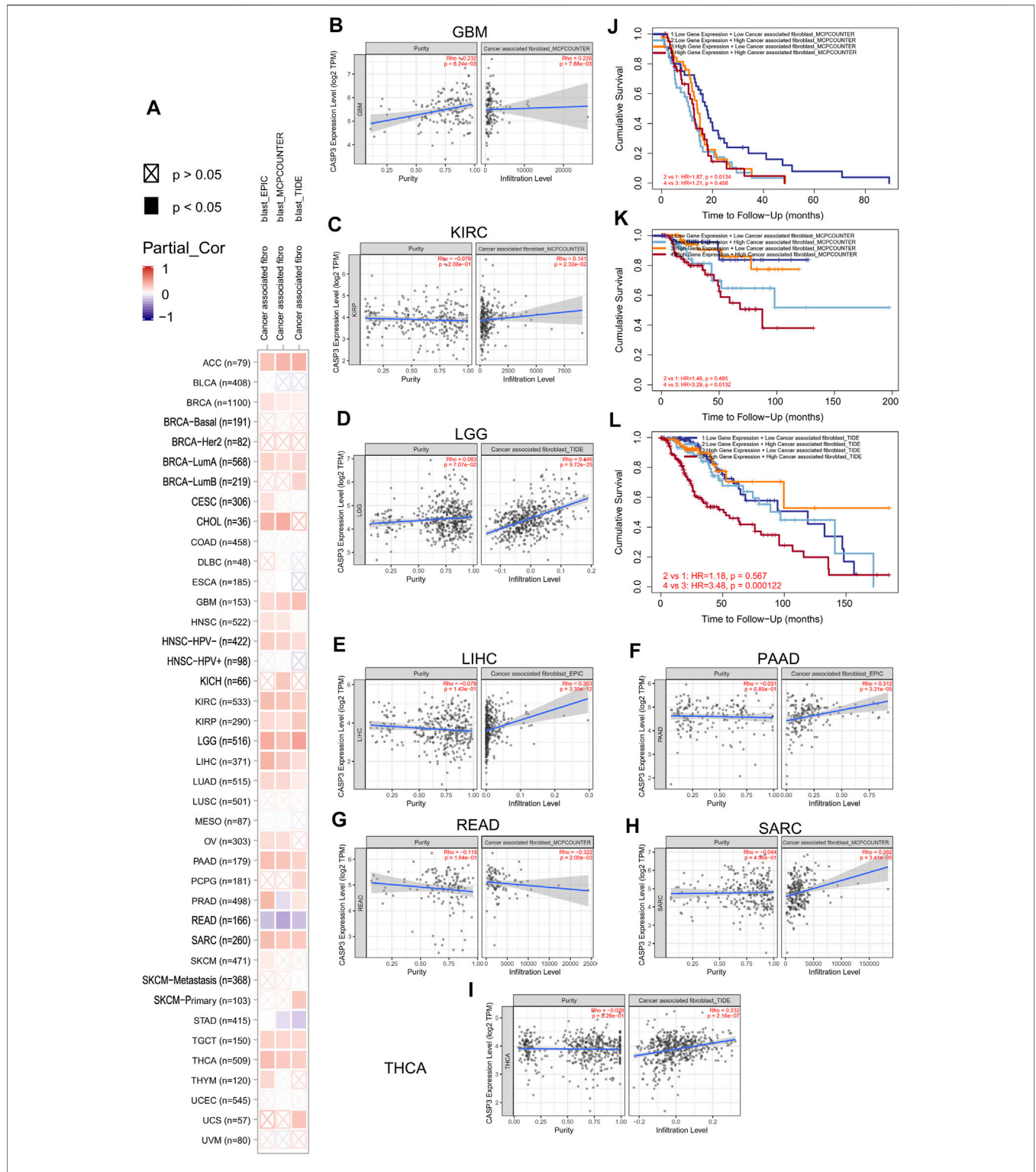


**FIGURE 8 |** Relationship between the expression of *CASP3* and cancer-associated fibroblasts infiltration. **(A)** Relationship between expression of *CASP3* and infiltration of 33 kinds of cancer-associated fibroblasts based on three algorithms. **(B–I)** expression of *CASP3* in GBM, KIRC, LGG, LIHC, PAAD, READ, SARC, THCA and its correlation with fibroblasts infiltration. **(J–L)** Kaplan-Meier survival analysis of *CASP3* gene expression and fibroblasts infiltration in relation to OS of GBM, KIRC and LGG.

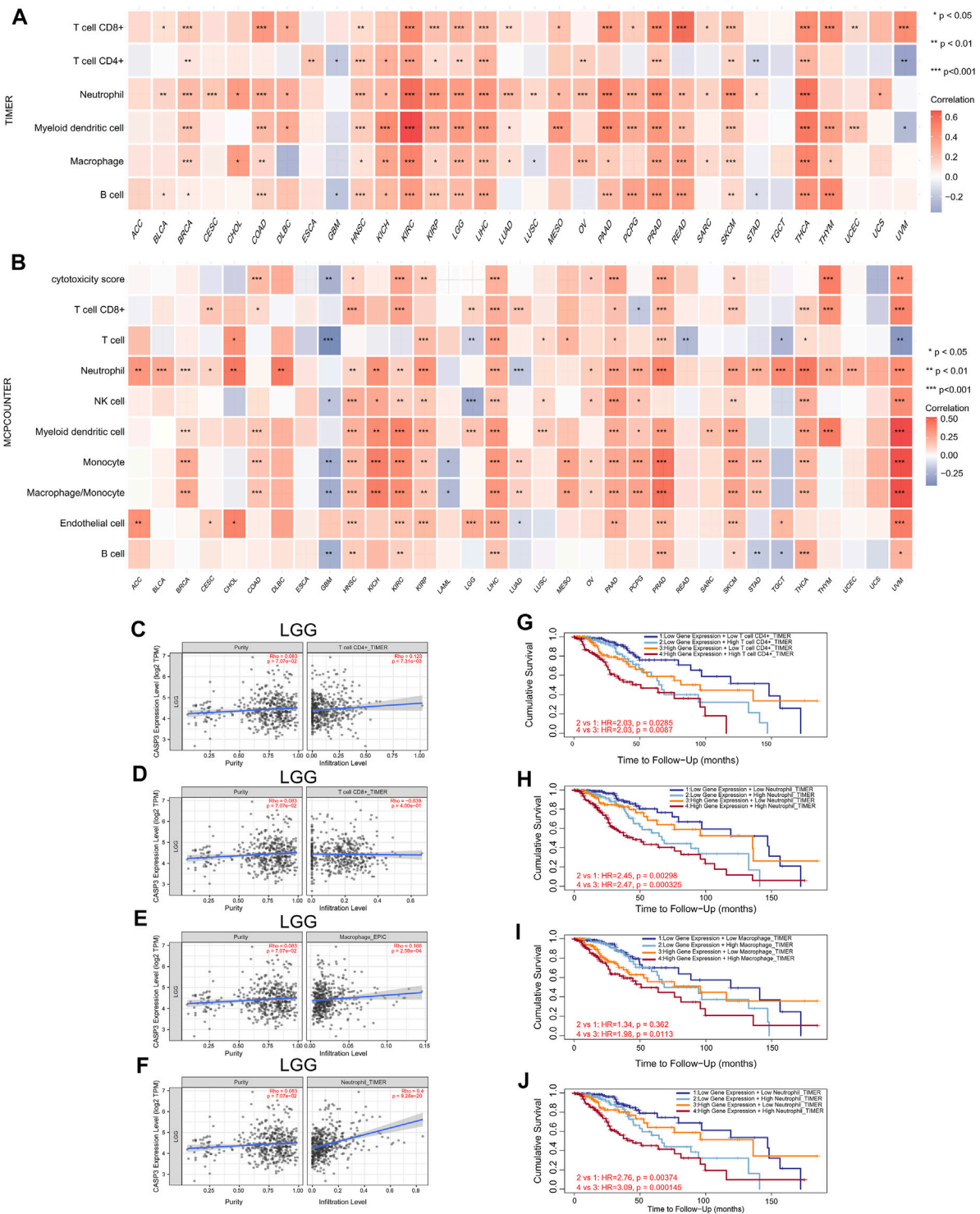


**FIGURE 9 |** Relationship between the expression of CASP3 and tumour immune cell infiltration. **(A)** Correlation between expression of CASP3 based on TIMER algorithm and tumour immune cell infiltration. \* $p < 0.05$ , \*\* $p < 0.01$ , \*\*\* $p < 0.001$ . **(B)** Correlation between the expression of CASP3 based on MCP-counter algorithm and tumour immune cell infiltration. \* $p < 0.05$ , \*\* $p < 0.01$ , \*\*\* $p < 0.001$ . **(C–F)** Relationship between the expression of CASP3 in LGG and the infiltration of immune cells. **(G–J)** Kaplan-Meier survival analysis of CASP3 expression and the relationship between immune infiltration and OS of LGG.

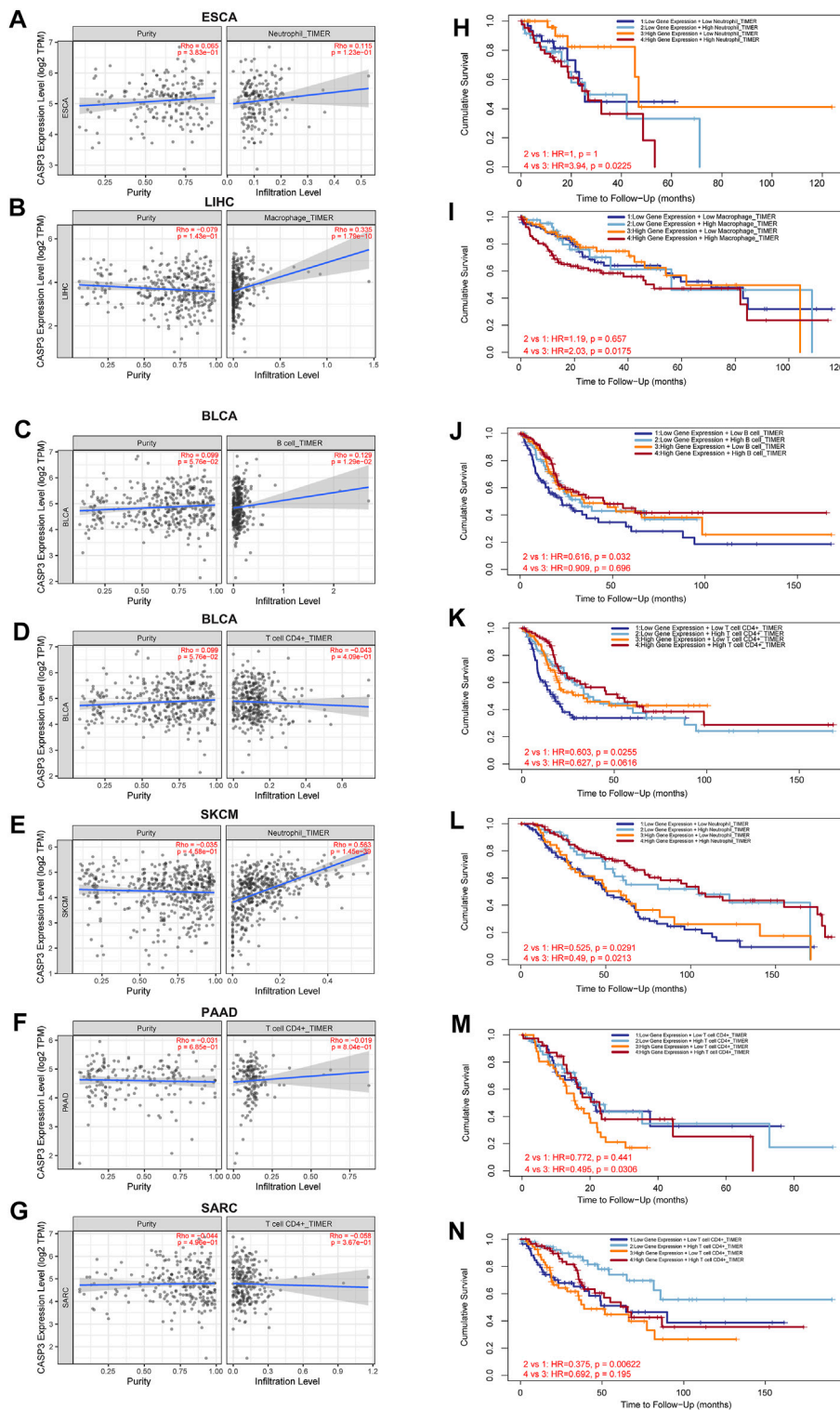


**FIGURE 10 |** Relationship between *CASP3* expression and tumour immune cell infiltration. (A–G) the expression of *CASP3* in ESCA, LIHC, BLCA, skin cutaneous melanoma (SKCM), PAAD, SARC and its relationship with immune cell infiltration. (H–N) Kaplan-Meier survival analysis of *CASP3* expression and the relationship between immune infiltration and OS of ESCA, LIHC, BLCA, SKCM, PAAD, SARC.



## Tumour Microenvironment Analysis Data

We first analysed the correlation between *CASP3* and eight immunologic checkpoint-related genes in all tumours. *CASP3* expression was negatively correlated ( $p < 0.05$ ) with these immunologic checkpoint-related genes in all tumours, except in ACC, GBM, THYM, and TGCT (Figure 7C). Thereafter, the tumour microenvironment was analysed. Tide, MCP-counter, and EPIC algorithms were selected using TIMER2's "Associated cancer fibroblast" module to analyse the relationship between *CASP3* expression and fibroblast infiltration in different TCGA tumours. *CASP3* expression was positively correlated with the invasion of fibroblasts in ACC, BRCA-lumA, HNSC-HPV, GBM, KIRC, KIRP, LGG, LIHC, LUAD, PAAD, SARC, TGCT, and THCA, but was negatively correlated with fibroblast infiltration in READ (Figure 8A); the relevant scatter plots are shown in Figures 8D–I. We further analysed the effects of *CASP3* expression and fibroblast infiltration on tumour prognosis. We chose the algorithm with obvious differences in prognosis; in turn, in GBM, KIRP, and LGG, poor prognosis was observed when fibroblasts were highly infiltrating (Figures 7J,K). The remaining relevant scatter plots are shown in Supplementary Figure S3.

Next, TIMER, xCell, MCP-counter, CIBERSORT, EPIC, and QUANTISEQ algorithms were used to investigate the potential relationship between the invasion level of different immune cells and *CASP3* expression in different cancer types in TCGA. Based on MCP-counter and TIMER algorithm data, we found that, almost all other tumours in the presence of *CASP3* expression was positively correlated with relevant immune cell infiltration in almost all tumours, with exception of ACC, GBM, and TGCT (Figures 9A,B). Based on several algorithms, we found that *CASP3* expression was closely related to the immune invasion of many cell types. We selected the TIMER algorithm and analysed the prognostic correlation. The scatter plots and Kaplan-Meier survival curve are shown in Figures 9C–J. Increased numbers of CD4<sup>+</sup> T cells, CD8<sup>+</sup> T cells, neutrophils, and macrophages in LGG were associated with poorer prognosis. High neutrophil infiltration in ESCA and high macrophage infiltration in LIHC were also associated with poor prognosis (Figures 10A–N). In BLCA, increased numbers of CD4<sup>+</sup> T cells and B cells indicated an improved prognosis, and increased neutrophil infiltration in SKCM and increased CD4<sup>+</sup> T cell infiltration in PAAD and SARC also predicted improved prognosis. The correlation scatter plots of the remaining tumours are shown in Supplementary Figure S4.

## Enrichment Analysis Data

We performed GSEA to investigate the biological significance of *CASP3* expression in different tumours from TCGA. The results based on KEGG and GO are shown in Figures 11A–Q. In KEGG enrichment analysis, *CASP3* expression in CHOL, LGG, OV, PRAD, THYM, and THCA was related to autophagy regulation, cytosolic DNA sensing pathway, cytokine receptor interaction, ascorbate and aldarate metabolism, neuroactive ligand receptor interaction, and porphyrin and chlorophyll metabolism, and mostly occurred through positive regulation, although it occurred through a negative regulation in STAD. These

included related pathways that were positively regulated in most tumours, such as autophagy regulation and cytosolic DNA sensing pathway. Further, *CASP3* expression in OV and TGCT was positively regulated by antigen presentation and processing. In GO analysis, *CASP3* was most strongly associated with the detection of chemical stimulus pathways in almost all tumours, including the sensory perception of smell, olfactory receptor activity, and mRNA binding. These pathways were positively regulated in BLCA, ESCA, HNSC, and DLBC, and negatively regulated in STAD, LUSC, PRAD, and READ. However, the result of *CASP3* expression in OV in GO was the same as that in KEGG, indicating the involvement in B cell activation and immune response-regulating signalling pathways. *CASP3* also participates in the CCR chemokine receptor binding pathway and produces positive regulation in DLBC. The remaining tumour-associated GO enrichment analysis is shown in Supplementary Figure S5.

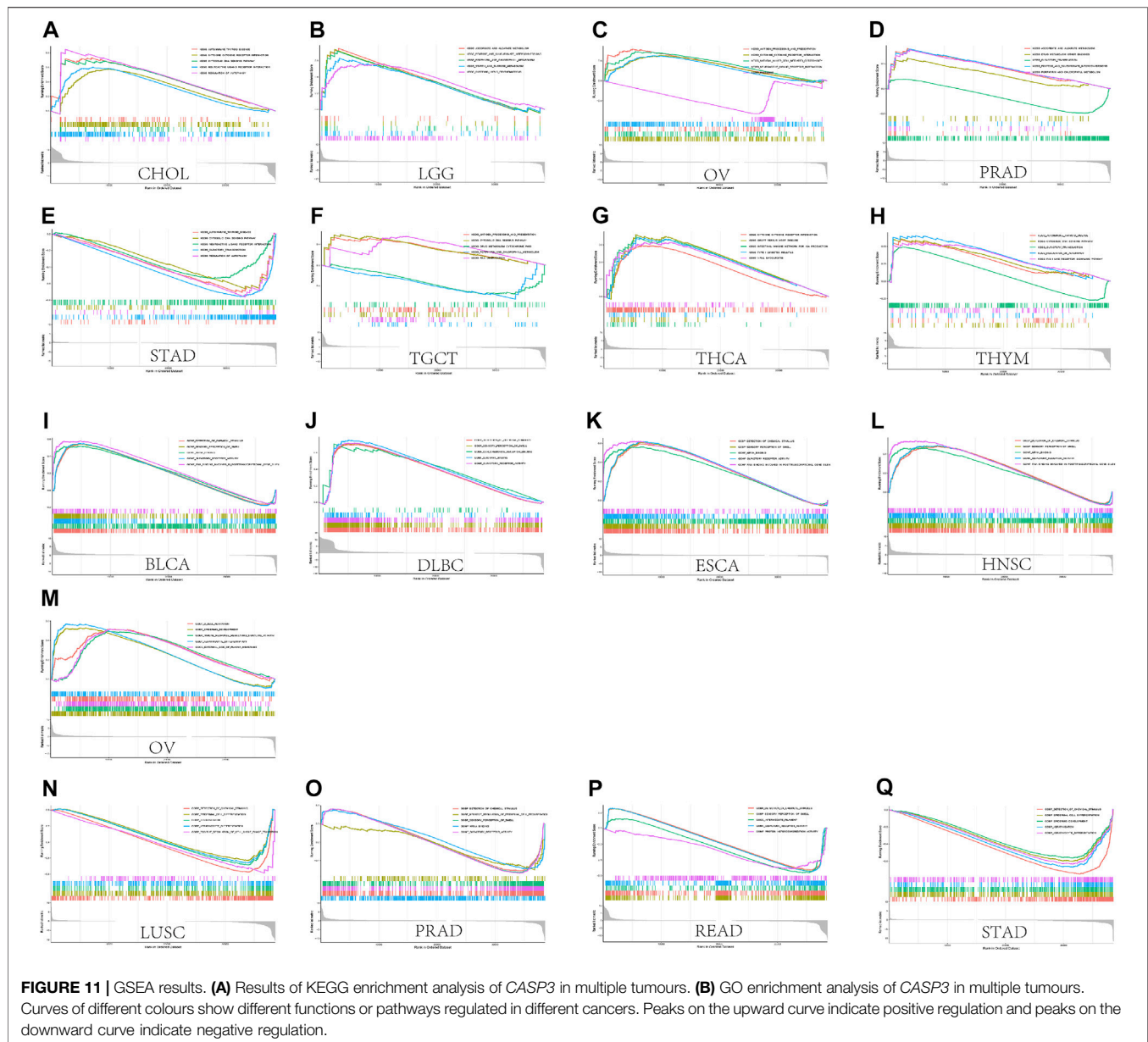
## CASP3-Related Gene Enrichment Analysis Data

To further investigate the mechanism of *CASP3* in tumorigenesis and cancer progression, the first 100 genes related to *CASP3* expression were obtained from all tumour expression data in TCGA using GEPIA2. A heatmap of the correlation is shown in Figure 12A. In addition, we screened 50 *CASP3*-binding proteins from the STRING website, supported by experimental data, as shown in Figure 12B. The expression of *DDX46* ( $R = 0.46$ ), *GNAI3* ( $R = 0.56$ ), *PDS5A* ( $R = 0.57$ ), *SCYL2* ( $R = 0.51$ ), and *TMPO* ( $R = 0.63$ ) were positively correlated with the *CASP3* levels ( $p < 0.001$ , Figures 12C–G). We then combined the two datasets for KEGG and GO enrichment analyses. According to the KEGG results (Figures 12H,I), in addition to apoptosis, *CASP3* may play a role in the tumour through infection and as a spliceosome. GO enrichment analysis data (Figures 12J,K) further showed that most of these genes affect cell biology by regulating the activities of apoptosis-related proteases, including peptidase and endopeptidase.

## DISCUSSION

In recent years, an increasing number of studies have reported that *CASP3* is involved in cellular biological processes that cannot be defined simply by apoptosis; however, whether it is clinically relevant, and whether different tumours perform the same or different functions through the same molecular mechanism, remains unknown. A literature search failed to obtain any publications that analysed *CASP3* from the pan-cancer perspective. Therefore, we analysed the *CASP3* in 33 different tumours using the TCGA, CPTAC, and GTEx databases by investigating gene expression, genetic changes, gene methylation, and other molecular characteristics.

Our findings showed increased *CASP3* expression in 31 tumours in the TCGA database, 16 of which were statistically significant ( $p < 0.05$ ), which was also demonstrated by protein expression analysis. In the meantime, we're trying to find some



clinical evidence that continues to support our view. Unfortunately, most studies have not studied the role of *CASP3* in related tumour tissues, the Caspase-3 protein has been used as a target in most of the researches.

However, Kaplan-Meier survival analysis of the *CASP3* relationship showed a different result. For OS, we used GEPIA2 to analyse the statistical correlation between *CASP3* overexpression and overall survival outcomes, but our results differed from those obtained previously. We observed a significant correlation between *CASP3* overexpression and poor prognosis in ACC and LGG. The reason for this difference may be related to different data processing and analysis methods used. In addition, with the expression of *CASP3* in different tumours, the relationship between *CASP3* expression and survival may even appear to the contrary, which

suggests that we need specific tumour analysis in the study of the relationship between *CASP3* expression and prognosis. In our analysis, we found that the expression of *CASP3* in HNSC and STAD was positively correlated with age and sex ( $p < 0.05$ , **Supplementary Figure S6**). This is consistent with previous findings (Huang et al., 2018) and may have important implications for guiding clinical immunotherapy regimens in the future.

DNA methylation is an important epigenetic mechanism that controls cell proliferation, apoptosis, differentiation, cell cycle, and transformation in eukaryotes, and many cancers are associated with promoter-specific hypermethylation (Morgan et al., 2018). Results from existing studies indicate that DNA methylation levels can be used as biomarkers for the early detection, diagnosis, and prognosis of cancer (Pan et al.,

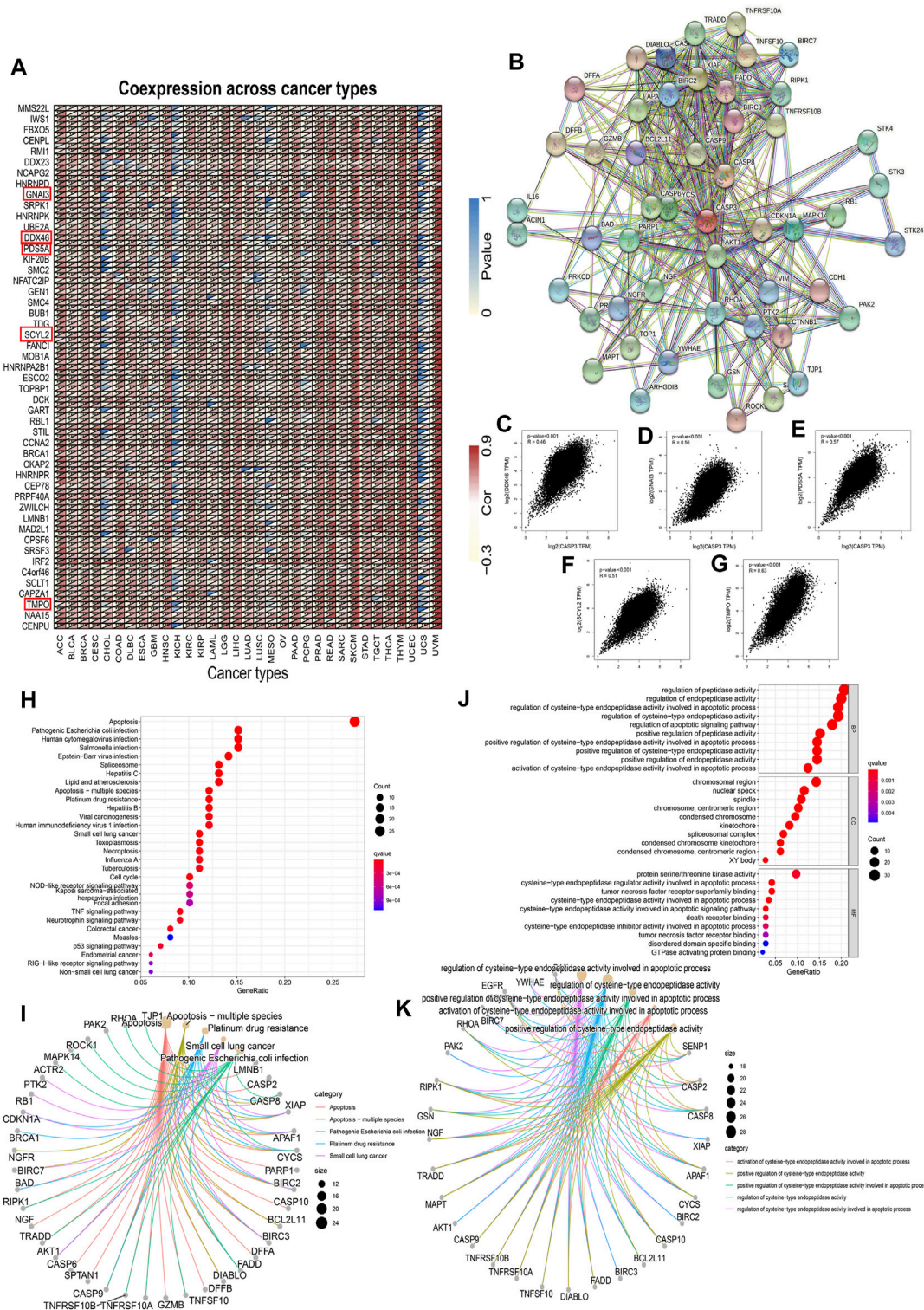


**FIGURE 12 | CASP3-related gene enrichment analysis. (A)** Relationship between the *CASP3* and the first 100 genes in different tumours. The triangle in the upper left corner represents the *p*-value, and the triangle in the lower right corner represents the correlation coefficient. \**p* < 0.05, \*\**p* < 0.01, \*\*\**p* < 0.001. **(B)** Interaction of *CASP3* with the binding protein of the first 50. **(C–G)** Relationship between *CASP3* and the expression of selected genes (*DDX46*, *GNAI3*, *PDS5A*, *SCYL2*, *TMPO*) **(H,I)** based on *CASP3*-binding and correlated gene KEGG enrichment analysis results, and **(J,K)** based on *CASP3*-binding and correlated gene GO enrichment analysis results.

2018). We investigated, for the first time, the relationship between the methylation level of *CASP3* and different tumours, and its effect on clinical prognosis. Except for tumours without related methylation and prognosis data, significant results were obtained for clinical survival and prognosis. Therefore, we can conclude that the *CASP3* methylation level can be used as an independent prognostic factor for tumours. However, there are still few studies on the methylation of *CASP3*, which seems to be a promising direction in the future.

Recently, several studies have shown that *CASP3* expression often plays a role in tumours by participating in the pyroptosis process (Yu et al., 2019; Zhang et al., 2019), which is a type of programmed cell death in the form of inflammation, initially believed to be associated with innate immunity (Jorgensen and Miao, 2015). Subsequent studies have shown that pyroptosis in tumours can inhibit the proliferation and migration of tumour cells and, thus, affect prognosis (Fang et al., 2020). Therefore, we investigated the relationship between *CASP3* expression and immunity.

Both TMB and MSI are closely related to the tumour microenvironment and immunotherapy; hence, have recently received increasing attention. Recent studies have identified TMB as a biomarker for immunotherapy (Chan et al., 2019), as is considered to specifically affect immunotherapy outcomes by increasing the production of proteins recognised by the immune system in patients with high TMB. Immune cells are more likely to recognise and clear tumour cells with high TMB (Chen and Mellman, 2017; Chan et al., 2019). In patients with colorectal cancer, the sensitivity of MSI-high to immunologic checkpoint inhibitors (ICIs) is significantly higher than that of MSI-low (Lin et al., 2020). Herein, we found that *CASP3* expression in READ was closely related to MSI ( $p = 0.001$ ). Studies have confirmed that the use of ICIs for treating tumours has become increasingly important in tumour immunotherapy (Darvin et al., 2018), and subsequent analysis of the correlation of immunologic checkpoints also revealed that *CASP3* plays a significant role in tumours. It is thus reasonable to conclude that tumours with high *CASP3* expression and positive association with TMB and MSI would be more sensitive to ICI therapy, which suggests an improved immunotherapy prognosis.

Tumour-infiltrating immune cells and cancer-associated fibroblasts in the tumour matrix, which are important components of the tumour microenvironment, are closely related to cancer occurrence, development, and metastasis (Lei et al., 2020), and targeted therapy of the tumour microenvironment has become the focus of the current research for anticancer therapies (Xiao and Yu, 2021). Our follow-up findings on the role of *CASP3* in immunologic invasion, especially in  $CD8^+$  T cells, are consistent with previous studies (Jaime-Sanchez et al., 2020; Morris et al., 2020). Our results indicate that *CASP3* expression is positively correlated with the immunologic invasion of most tumours and has wide tumour practicability. Tumour-infiltrating immune cells play an important role in inhibiting or promoting tumorigenesis and cancer progression (Lei et al., 2020). Moreover, our results indicate a relationship between different immune cell infiltration and prognosis in different tumours; for example, in LGG, high *CASP3* expression and high infiltration of most immune cells were associated with poor prognosis, which provides a new direction for future research on ICIs. However, in BLCA, the

results were reversed, which is consistent with previous studies (Zhang et al., 2020). Furthermore, increased fibroblast infiltration is reported to support the growth, movement, and invasion of tumour cells, resulting in tumour development and metastasis (Kuzet and Gaggioli, 2016). To the best of our knowledge, our study is the first to demonstrate the relationship between *CASP3* expression and fibroblast infiltration in tumours and to reveal its association with poor prognosis. However, it is a pity that we try to further explore the relationship between cancer-associated fibroblast subpopulations and tumour, but we find that there is a lack of relevant research data.

The results of tumour enrichment and co-expression enrichment analyses were similar. In addition to apoptosis, the possible mechanisms of *CASP3* action may involve B cell activation, antigen presentation, immune responses, chemokine receptors, and inflammatory function, which is consistent with previous studies indicating that *CASP3* is a key protein in the regulation of tumour progression in addition to pyroptosis (Jiang et al., 2020). The enriched TNF and p53 signalling pathways in the KEGG bubble plot have also been studied to confirm that *CASP3* plays an important role in the pyroptosis process in tumours (Wang et al., 2017; Wang et al., 2021).

## CONCLUSION

In summary, our pan-cancer analysis of *CASP3* showed a statistically significant association between gene expression and clinical prognosis, DNA methylation, gene mutations, tumour microenvironment, TMB, and MSI across multiple tumours, and possibly related molecular mechanisms, with carryable outcomes depending on the tumour type. Our study has some limitations, such as the unevaluated drug sensitivity of *CASP3* expression to ICIs and lacks experimental validation. However, to the best of our knowledge, this study is the first to explore the relationship between *CASP3* methylation in different tumours and the tumour microenvironment, along with the effect of these two factors on prognosis. These findings can help to further clarify the role of *CASP3* in tumorigenesis and development and provide a new reference for potential applications in immunotherapy.

## DATA AVAILABILITY STATEMENT

The datasets presented in this study can be found in online repositories. The names of the repository/repositories and accession number(s) can be found in the article/**Supplementary Material**.

## AUTHOR CONTRIBUTIONS

ZZ contributed to conception and design of the study. ZZ organized the database and performed the statistical analysis. SX wrote the first draft of the manuscript. ZZ, SX, LJ, and ZT wrote sections of the manuscript. JW made revisions to the final manuscript. All authors contributed to manuscript revision, read, and approved the submitted version.

## FUNDING

This study was supported by the Medical and Health Science Research Fund of Zhejiang Province (2021KY055) and the Scientific Research Fund of Traditional Chinese Medicine of Zhejiang Province (2021ZA008).

## SUPPLEMENTARY MATERIAL

The Supplementary Material for this article can be found online at: <https://www.frontiersin.org/articles/10.3389/fmolb.2022.776808/full#supplementary-material>

## REFERENCES

- Bernard, A., Chevrier, S., Beltjens, F., Dosset, M., Viltard, E., Lagrange, A., et al. (2019). Cleaved Caspase-3 Transcriptionally Regulates Angiogenesis-Promoting Chemotherapy Resistance. *Cancer Res.* 79 (23), 5958–5970. doi:10.1158/0008-5472.CAN-19-0840
- Blum, A., Wang, P., and Zenklusen, J. C. (2018). SnapShot: TCGA-Analyzed Tumors. *Cell* 173 (2), 530. doi:10.1016/j.cell.2018.03.059
- Bonneville, R., Krook, M. A., Kautto, E. A., Miya, J., Wing, M. R., Chen, H.-Z., et al. (2017). Landscape of Microsatellite Instability across 39 Cancer Types. *JCO Precision Oncol.* 2017, 1–15. doi:10.1200/PO.17.00073
- Bulk, J. V. D., Verdegaal, E. M., and de Miranda, N. F. (2018). Cancer Immunotherapy: Broadening the Scope of Targetable Tumours. *Open Biol.* 8 (6), 180037. doi:10.1098/rsob.180037
- Chan, T. A., Yarchoan, M., Jaffee, E., Swanton, C., Quezada, S. A., Stenzinger, A., et al. (2019). Development of Tumor Mutation Burden as an Immunotherapy Biomarker: Utility for the Oncology Clinic. *Ann. Oncol.* 30 (1), 44–56. doi:10.1093/annonc/mdy495
- Chen, D. S., and Mellman, I. (2017). Elements of Cancer Immunity and the Cancer-Immune Set point. *Nature* 541 (7637), 321–330. doi:10.1038/nature21349
- Crowley, L. C., and Waterhouse, N. J. (2016). Detecting Cleaved Caspase-3 in Apoptotic Cells by Flow Cytometry. *Cold Spring Harb Protoc.* 2016 (11), pdb.prot087312. doi:10.1101/pdb.prot087312
- Darvin, P., Toor, S. M., Sasidharan Nair, V., and Elkord, E. (2018). Immune Checkpoint Inhibitors: Recent Progress and Potential Biomarkers. *Exp. Mol. Med.* 50 (12), 1–11. doi:10.1038/s12276-018-0191-1
- Fang, Y., Tian, S., Pan, Y., Li, W., Wang, Q., Tang, Y., et al. (2020). Pyroptosis: A New Frontier in Cancer. *Biomed. Pharmacother.* 121, 109595. doi:10.1016/j.biopha.2019.109595
- Feng, X., Yu, Y., He, S., Cheng, J., Gong, Y., Zhang, Z., et al. (2017). Dying Glioma Cells Establish a Proangiogenic Microenvironment through a Caspase 3 Dependent Mechanism. *Cancer Lett.* 385, 12–20. doi:10.1016/j.canlet.2016.10.042
- Huang, K.-H., Fang, W.-L., Li, A. F.-Y., Liang, P.-H., Wu, C.-W., Shyr, Y.-M., et al. (2018). Caspase-3, a Key Apoptotic Protein, as a Prognostic Marker in Gastric Cancer after Curative Surgery. *Int. J. Surg.* 52, 258–263. doi:10.1016/j.ijsu.2018.02.055
- Jaime-Sanchez, P., Uranga-Murillo, I., Aguilo, N., Khouli, S. C., Arias, M. A., Sancho, D., et al. (2020). Cell Death Induced by Cytotoxic CD8+T Cells Is Immunogenic and Primes Caspase-3-dependent Spread Immunity against Endogenous Tumor Antigens. *J. Immunother. Cancer* 8 (1), e000528. doi:10.1136/jitc-2020-000528
- Jiang, M., Qi, L., Li, L., and Li, Y. (2020). The Caspase-3/GSDME Signal Pathway as a Switch between Apoptosis and Pyroptosis in Cancer. *Cell Death Discov.* 6, 112. doi:10.1038/s41420-020-00349-0
- Jorgensen, I., and Miao, E. A. (2015). Pyroptotic Cell Death Defends against Intracellular Pathogens. *Immunol. Rev.* 265 (1), 130–142. doi:10.1111/imr.12287
- Kuzet, S.-E., and Gaggioli, C. (2016). Fibroblast Activation in Cancer: when Seed Fertilizes Soil. *Cell Tissue Res* 365 (3), 607–619. doi:10.1007/s00441-016-2467-x
- Le, D. T., Uram, J. N., Wang, H., Bartlett, B. R., Kemberling, H., Eyring, A. D., et al. (2015). PD-1 Blockade in Tumors with Mismatch-Repair Deficiency. *N. Engl. J. Med.* 372 (26), 2509–2520. doi:10.1056/NEJMoa1500596
- Lei, X., Lei, Y., Li, J.-K., Du, W.-X., Li, R.-G., Yang, J., et al. (2020). Immune Cells within the Tumor Microenvironment: Biological Functions and Roles in Cancer Immunotherapy. *Cancer Lett.* 470, 126–133. doi:10.1016/j.canlet.2019.11.009
- Lin, A., Zhang, J., and Luo, P. (2020). Crosstalk between the MSI Status and Tumor Microenvironment in Colorectal Cancer. *Front. Immunol.* 11, 2039. doi:10.3389/fimmu.2020.02039
- Liu, X., He, Y., Li, F., Huang, Q., Kato, T. A., Hall, R. P., et al. (2015). Caspase-3 Promotes Genetic Instability and Carcinogenesis. *Mol. Cell* 58 (2), 284–296. doi:10.1016/j.molcel.2015.03.003
- Mattiuzzi, C., and Lippi, G. (2019). Current Cancer Epidemiology. *Jegh* 9 (4), 217–222. doi:10.2991/jegh.k.191008.001
- Morgan, A. E., Davies, T. J., and Mc Auley, M. T. (2018). The Role of DNA Methylation in Ageing and Cancer. *Proc. Nutr. Soc.* 77 (4), 412–422. doi:10.1017/S0029665118000150
- Morris, A. B., Farley, C. R., Pinelli, D. F., Adams, L. E., Cragg, M. S., Boss, J. M., et al. (2020). Signaling through the Inhibitory Fc Receptor FcγRIIB Induces CD8+ T Cell Apoptosis to Limit T Cell Immunity. *Immunity* 52 (1), 136–150. e6. doi:10.1016/j.immuni.2019.12.006
- Pan, Y., Liu, G., Zhou, F., Su, B., and Li, Y. (2018). DNA Methylation Profiles in Cancer Diagnosis and Therapeutics. *Clin. Exp. Med.* 18 (1), 1–14. doi:10.1007/s10238-017-0467-0
- Sturm, G., Finotello, F., and List, M. (2020). Immunedeconv: An R Package for Unified Access to Computational Methods for Estimating Immune Cell Fractions from Bulk RNA-Sequencing Data. *Methods Mol. Biol.* 2120, 223–232. doi:10.1007/978-1-0716-0327-7\_16
- Thorsson, V., Gibbs, D. L., Brown, S. D., Wolf, D., Bortone, D. S., Ou Yang, T. H., et al. (2018). The Immune Landscape of Cancer. *Immunity* 48 (4), 812. e14. doi:10.1016/j.immuni.2018.03.023
- Wang, X., Liu, K., Gong, H., Li, D., Chu, W., Zhao, D., et al. (2021). Death by Histone Deacetylase Inhibitor Quisinostat in Tongue Squamous Cell Carcinoma via Apoptosis, Pyroptosis, and Ferroptosis. *Toxicol. Appl. Pharmacol.* 410, 115363. doi:10.1016/j.taap.2020.115363
- Wang, Y., Gao, W., Shi, X., Ding, J., Liu, W., He, H., et al. (2017). Chemotherapy Drugs Induce Pyroptosis through Caspase-3 Cleavage of a Gasdermin. *Nature* 547 (7661), 99–103. doi:10.1038/nature22393
- Xiao, Y., and Yu, D. (2021). Tumor Microenvironment as a Therapeutic Target in Cancer. *Pharmacol. Ther.* 221, 107753. doi:10.1016/j.pharmthera.2020.107753
- Yarchoan, M., Hopkins, A., and Jaffee, E. M. (2017). Tumor Mutational Burden and Response Rate to PD-1 Inhibition. *N. Engl. J. Med.* 377 (25), 2500–2501. doi:10.1056/NEJMc1713444
- Yu, J., Li, S., Qi, J., Chen, Z., Wu, Y., Guo, J., et al. (2019). Cleavage of GSDME by Caspase-3 Determines Lobaplatin-Induced Pyroptosis in colon Cancer Cells. *Cell Death Dis* 10 (3), 193. doi:10.1038/s41419-019-1441-4
- Zhang, C.-c., Li, C.-g., Wang, Y.-f., Xu, L.-h., He, X.-h., Zeng, Q.-z., et al. (2019). Chemotherapeutic Paclitaxel and Cisplatin Differentially Induce Pyroptosis in A549 Lung Cancer Cells via Caspase-3/GSDME Activation. *Apoptosis* 24 (3–4), 312–325. doi:10.1007/s10495-019-01515-1

Zhang, C., Shen, L., Qi, F., Wang, J., and Luo, J. (2020). Multi-omics Analysis of Tumor Mutation burden Combined with Immune Infiltrates in Bladder Urothelial Carcinoma. *J. Cel Physiol* 235 (4), 3849–3863. doi:10.1002/jcp.29279

Zhou, M., Liu, X., Li, Z., Huang, Q., Li, F., and Li, C.-Y. (2018). Caspase-3 Regulates the Migration, Invasion and Metastasis of colon Cancer Cells. *Int. J. Cancer* 143 (4), 921–930. doi:10.1002/ijc.31374

**Conflict of Interest:** The authors declare that the research was conducted in the absence of any commercial or financial relationships that could be construed as a potential conflict of interest.

The reviewer ZW declared a shared parent affiliation with the author(s) to the handling editor at the time of review.

**Publisher's Note:** All claims expressed in this article are solely those of the authors and do not necessarily represent those of their affiliated organizations, or those of the publisher, the editors and the reviewers. Any product that may be evaluated in this article, or claim that may be made by its manufacturer, is not guaranteed or endorsed by the publisher.

*Copyright © 2022 Zhou, Xu, Jiang, Tan and Wang. This is an open-access article distributed under the terms of the Creative Commons Attribution License (CC BY). The use, distribution or reproduction in other forums is permitted, provided the original author(s) and the copyright owner(s) are credited and that the original publication in this journal is cited, in accordance with accepted academic practice. No use, distribution or reproduction is permitted which does not comply with these terms.*